EGFRvIV: a previously uncharacterized oncogenic mutant reveals a kinase autoinhibitory mechanism

G Pines[1], **PH Huang**[2,3], **Y Zwang**[1], **FM White**[2], and **Y Yarden**[1]

[1]Department of Biological Regulation, The Weizmann Institute of Science, Rehovot, Israel

[2]Department of Biological Engineering, Massachusetts Institute of Technology, Cambridge, MA, USA

Abstract

Tumor cells often subvert normal regulatory mechanisms of signal transduction. This study shows this principle by studying yet uncharacterized mutants of the epidermal growth factor receptor (EGFR) previously identified in glioblastoma multiforme, which is the most aggressive brain tumor in adults. Unlike the well-characterized EGFRvIII mutant form, which lacks a portion of the ligand-binding cleft within the extracellular domain, EGFRvIVa and EGFRvIVb lack internal segments distal to the intracellular tyrosine kinase domain. By constructing the mutants and by ectopic expression in naive cells, we show that both mutants confer an oncogenic potential in vitro, as well as tumorigenic growth in animals. The underlying mechanisms entail constitutive receptor dimerization and basal activation of the kinase domain, likely through a mechanism that relieves a restraining molecular fold, along with stabilization due to association with HSP90. Phospho-proteomic analyses delineated the signaling pathways preferentially engaged by EGFRvIVb-identified unique substrates. This information, along with remarkable sensitivities to tyrosine kinase blockers and to a chaperone inhibitor, proposes strategies for pharmacological interception in brain tumors harboring EGFRvIV mutations.

Keywords

EGFR mutations; glioblastoma; growth factor; signal transduction; tyrosine kinase

Introduction

Growth factors and their receptors control cell-fate decisions, including survival, differentiation, proliferation or migration, and hence they have critical roles in hyperproliferative diseases, including malignancies (Hynes and MacDonald, 2009). Increased availability of growth factors because of either autocrine or paracrine loops and genetically aberrant forms of the respective cell surface receptors, or their downstream signaling components, are frequently detected in tumors. A striking example is provided by the epidermal growth factor (EGF) and the cognate receptor (EGFR, also termed ErbB-1). The extracellular portion of EGFR is composed of two cysteine-rich domains that form the ligand-binding cleft (Burgess *et al.*, 2003), whereas the intracellular portion consists of a

Correspondence: Professor Y Yarden, Department of Biological Regulation, Candiotty Building (Room 302), The Weizmann Institute of Science, 1 Hertzl Street, Rehovot 76100, Israel. yosef.yarden@weizmann.ac.il.
[3]Current address: Section of Cell and Molecular Biology, Institute of Cancer Research, London, UK.

Conflict of interest
The authors declare no conflict of interest.

juxtamembrane and a tyrosine kinase domain, followed by a distal carboxyl tail (C-tail) that undergoes autophosphorylation. Upon ligand binding and consequent kinase activation, EGFR activates several downstream signaling cascades, such as the mitogen-activated protein kinase cascade and the phosphoinositol 3-kinase pathway (Katz *et al.*, 2007).

EGFR is commonly overexpressed or mutated in human malignancies, and a close examination of the mutated areas clearly indicates that these mutations are not randomly dispersed along the receptor, but are rather concentrated in specific 'hot spots' (Ladanyi and Pao, 2008). Not surprisingly, these frequently mutated domains encompass well-defined regulatory elements that prevent untimely stimulation of the highly mitogenic downstream signaling pathways. For example, EGFRvIII, a deletion mutant lacking exons 2–7, including a portion of the extracellular ligand-binding domain, is commonly found in glioblastoma multiforme, which is an aggressive form of adult human brain tumors. Approximately 50% of glial tumors harbor EGFR gene amplification that correlates with receptor overexpression (Wong *et al.*, 1987), and a large fraction of these also present EGFRvIII (Jeuken *et al.*, 2009). Despite its inability to bind soluble ligands, EGFRvIII shows constitutive tyrosine phosphorylation and activation of multiple downstream signaling pathways (Huang *et al.*, 2009). Indeed, EGFRvIII molecules are basally dimerized and confer a high tumorigenic potential (Nagane *et al.*, 1996).

Other, less frequent deletion mutations were identified in glioblastoma multiforme. These mutated receptors present intracellular deletions, but their oncogenic potential remains hitherto uncharacterized. The carboxyl terminal deletion mutants, collectively termed EGFRvIV, lack either three exons (numbered 25–27; hereinafter EGFRvIVa) or two exons (25 and 26; hereinafter EGFRvIVb) (Ekstrand *et al.*, 1992; Frederick *et al.*, 2000; Kuan *et al.*, 2001), with the deletion initiating immediately downstream to the kinase domain. In this study we provide the first evidence for the transforming and tumorigenic properties of carboxyl terminal EGFR deletions. We show that the deletion mutants show ligand-independent constitutive activation, which engages distinct phosphorylation substrates. Importantly, the oncogenic function of EGFR harboring these carboxyl terminal deletions depends upon the intrinsic kinase activity and the chaperoning function of heat shock protein 90 (HSP90). Thus, beyond the demonstration of a novel kinase regulatory mechanism that depends on a specific carboxyl terminal segment, our findings suggest therapeutic strategies using EGFR-specific tyrosine kinase inhibitors, and/or HSP90 inhibitors, to target tumors harboring the EGFRvIV mutations.

Results

EGFRvIV can transform murine fibroblasts

To investigate the putative transforming potentials of the two EGFRvIV mutant forms (see schematic domain structures in Figure 1a), we constructed the respective retroviral expression vectors and stably expressed them, along with wild-type (WT) EGFR and the EGFRvIII mutant, in NIH-3T3 murine fibroblasts. Drug (G418)-resistant cell pools stably expressing these mutants gained phenotypes consistent with malignant transformation: cells expressing the mutants showed more rapid proliferation than cells that were infected either with an empty vector or with a WT-EGFR-encoding vector (Figure 1b). Another feature of the transformed phenotype, namely altered morphology of NIH-3T3 cells (Pulciani *et al.*, 1982), paralleled the differences in proliferation rates (Figure 1c): unlike control cells and cells expressing WT-EGFR, which preserved normal morphology, the shapes showed by EGFRvIV-expressing cells were consistent with transformation. Importantly, whereas the morphology of RAS-transformed cells was not affected by an EGFR-specific kinase inhibitor (AG1478), treatment with AG1478 largely reversed the morphological alterations associated with all three mutant forms of EGFR. These observations imply dependence of

the mutant receptors on the intrinsic catalytic activity for the acquisition of transformed phenotypes.

In line with accelerated cell proliferation and altered morphology, expression of the EGFRvIVb mutant conferred anchorage-independent growth of cell colonies in a semisolid (soft agar) medium (Figure 1d), a feature commonly showed by cancer cells. This property was shared by the EGFRvIII mutant, but not by WT-EGFR. Moreover, upon subcutaneous injection into nude mice, in contrast to WT-EGFR and NeoR cells, cells expressing either EGFRvIVa or EGFRvIVb formed tumors, although smaller than those formed by cells expressing the EGFRvIII mutant (Figure 1e). Although the shorter deletion of EGFRvIVb resulted in stronger transforming activity than EGFRvIVa, both mutants reflect the growth inhibitory roles of the C-tail, segments of which are deleted in brain tumors.

The EGFRvIV mutants are basally phosphorylated

Immunoblotting of tumor specimens derived from the xenografts grown subcutaneously in mice showed that tumors driven by all three EGFR deletion mutants showed detectable levels of tyrosine phosphorylation (inset in Figure 1e). This observation, along with the ability of an EGFR kinase inhibitor to reverse the transformed morphology of mutant-expressing cells (Figure 1c), raised the possibility that constitutive (ligand-independent) enzymatic activity of the mutant receptors underlies their tumorigenic properties. To examine this scenario we analyzed the state of receptor phosphorylation in whole extracts prepared from the cells shown in Figure 1c. Although WT-EGFR presented no tyrosine phosphorylation in the stably expressing murine fibroblasts, all deletion mutants showed detectable tyrosine phosphorylation, which was entirely lost upon treatment with AG1478 (Figure 2a). To further investigate the basal phosphorylation state of the mutants, as well as their relationships to EGF-induced phosphorylation, the status of several tyrosine residues was examined using antibodies specific to tyrosine-phosphorylated sites of EGFR. This analysis confirmed high basal phosphorylation of several major tyrosine residues (Figure 2b). Interestingly, treatment with EGF significantly enhanced phosphorylation of both EGFRvIV mutant forms. However, as expected, phosphorylation of EGFRvIII was not affected by the ligand (Figure 2b). Using transient expression of EGFRvIVb in human embryonic kidney (HEK)-293 human kidney cells, a system allowing very high expression levels, we confirmed basal tyrosine phosphorylation of the mutant at all doses of the transfected plasmid (Supplementary Figure S1). In contrast, the WT form of EGFR showed basal phosphorylation only when expressed at very high levels.

To validate the presence of relatively large populations of basally phosphorylated EGFRvIV mutant receptors in comparison to WT-EGFR, as well as to map the overall phosphoproteome differences, we applied LC/MS/MS (liquid chromatography tandem mass spectrometry) methods on extracts isolated from the NIH-3T3 cells ectopically expressing the different forms of EGFR. In brief, cells were either unstimulated or treated with EGF. Proteins present in cell extracts were digested and labeled and tyrosine-phosphorylated peptides were isolated, as previously described (Zhang *et al.*, 2005; Huang *et al.*, 2007). MS/MS spectra were extracted and quantified and peptide sequences assigned to specific proteins. Unsupervised examination of the data revealed grouping of samples according to whether or not cells were exposed to EGF (Supplementary Figure S2 and Excel File). The only exception was EGFRvIII, which cannot bind EGF. To identify components of the signaling networks that were either shared or unique to each form of EGFR, a clustering analysis was performed on phosphopeptides detected under basal (unstimulated) conditions. This analysis identified three distinct clusters (Figure 2c). The first represents proteins highly phosphorylated in WTEGFR, but weakly modified in mutant-expressing cells (denoted cluster 1). Clusters 2 and 3 are enriched for tyrosine-phosphorylated proteins in EGFRvIVb- and EGFRvIII-expressing cells, respectively. Interestingly, EGFRvIVa showed

very low levels of phosphoproteins under unstimulated conditions. As seen in Figure 2d, all three EGFR phosphotyrosine sites we quantified by mass spectrometry were phosphorylated at significantly higher levels in the mutant-expressing cell lines compared with WT-EGFR under unstimulated conditions, in line with constitutive activation and the results obtained using immunoblots (Figures 2a and b).

Constitutive downstream signaling by the EGFRvIV mutants

It is notable that clusters 2 and 3 were derived from unstimulated cells, yet they contained several signaling proteins, suggesting that the respective mutants activate signaling pathways in the absence of ligands. Closer analyses of the data revealed mutation-specific signatures of phosphorylation substrates (Figures 3a and b). For example, EGFRvIVb (cluster 2) activated STAT3 (signal transducer and activator of transcription 3) to a greater extent compared with WT-EGFR, EGFRvIII or EGFRvIVa, whereas the EGFRvIII mutant (cluster 3) preferentially activated another family member, STAT5b. This differential STAT activation suggests that the mutants activate different cellular programs (Clarkson *et al.*, 2006). Similarly, the adaptor protein SHC, which physically interacts with active EGFR, was assigned to cluster 2, with increased phosphorylation by EGFRvIVb and decreased phosphorylation in the WT-EGFR- and EGFRvIII-expressing cells. The cluster corresponding to EGFRvIII, however, included three phosphorylation sites of phospholipase C-γ1 (Y771, Y783 and Y1253) and two phosphorylation sites of AXL (Y696 and Y860), a mitogenic receptor tyrosine kinase of gliomas (Hafizi and Dahlback, 2006). Taken together, the two distinct clusters imply that each mutation preferentially activates different downstream signaling pathways.

To further address the possibility that the relatively high basal kinase activity of the EGFRvIV mutants leads to constitutive downstream signaling, we focused on SHC and GRB2 (growth factor receptor-bound protein 2), the two major adaptors linking activated EGFR to the mitogen-activated protein kinase pathway. In response to stimulation of WT-EGFR by ligands such as EGF, the receptor forms physical complexes with both adaptors, as shown in Figure 3c. In the case of the EGFRvIV mutants, complex formation occurred even in the absence of a stimulating ligand, although larger fractions of GRB2 and SHC were physically recruited to EGFR on stimulation with EGF. Interestingly, neither EGFRvIII nor EGFRvVa (a very rare deletion mutant of brain tumors encompassing all amino acids distal to the kinase domain) showed complex formation with the adaptors, even in the presence of EGF (Figure 3c). Congruent with these results, we detected constitutive, although weak, activation of the mitogen-activated protein kinase extracellular signal-regulated kinases 1 and 2 (and of AKT) in unstimulated cells expressing the EGFRvIV mutants (Figure 3d). In contrast, cells expressing EGFRvIII showed constitutive activation of the AKT pathway, rather than the extracellular signal-regulated kinase pathway, in line with a previous report (Huang *et al.*, 2007), once again supporting our conclusion that distinct pathways are recruited by EGFRvIII and the EGFRvIV mutants.

One major and early outcome of EGFR activation is the induction of JUN, an oncogenic transcription factor that participates in the bipartite activator protein-1 complex (Zenz and Wagner, 2006). Accordingly, immunoblotting for JUN detected enhanced ligand-induced expression in fibroblasts expressing WT-EGFR (Figure 3e). Conversely, cells expressing the EGFRvIV or EGFRvIII mutant receptors showed similarly high levels of JUN in the absence of ligand stimulation. A further increase was achieved upon stimulation of the EGFRvIV mutants, but no reproducible induction was observed in the EGFRvIII mutant.

Along with activation by EGFR mutants of forward-acting effectors, we expected inactivation of restraining mechanisms. In line with this prediction, our mass spectrometry analyses detected in cluster 1 high basal tyrosine phosphorylation of EPHA2, a negative

regulator of EGFR (Li *et al.*, 2009), in WT-EGFR-expressing cells. However, this signal was lower in the three lines of mutant-expressing cells (Supplementary Excel File). Interestingly, EPHA2 was reported to be overexpressed in an unphosphorylated form in glioblastoma multiforme cells and tumors (Wykosky *et al.*, 2005). To validate differential tyrosine phosphorylation, we determined the state of EPHA2 modification (Figure 3f). The results confirmed that tyrosine phosphorylation of EPHA2 is significantly higher in WT-EGFR-expressing cells than in cells expressing either mutant of EGFR, in agreement with our mass spectrometry data. Interestingly, the control Neo-resistant cells also showed reduced EPHA2 phosphorylation levels (Figure 3f), suggesting that EGFR is essential for phosphorylation of EPHA2, but this restraining module is defected by activating EGFR mutations.

Constitutive dimerization may underlie the basal phosphorylation of the EGFRvIV mutant receptors

To investigate the mechanism that underlies basal phosphorylation of the EGFRvIV mutants, we tested whether this basal activity was due to intrinsic activation or to enhanced sensitivity to autocrine stimulation by EGF-like ligands, as previously proposed (Ramnarain *et al.*, 2006). To test the autocrine alternative, stably expressing NIH-3T3 cells were treated with increasing EGF concentrations (Figure 4a). Quantification of the results showed a linear response of WT-EGFR phosphorylation to increasing, relatively low (<1.0 ng/ml) ligand concentrations (Figure 4b). Conversely, EGFR-vIVb was not responsive at this range of ligand concentrations, yet showed consistent basal activity, and underwent enhanced phosphorylation upon treatment with higher ligand concentrations (Figures 4a and b). This observation implies that enhanced sensitivity to EGF may not be the cause for the relatively high basal phosphorylation observed with the EGFRvIV mutants. Instead, the enhanced basal phosphorylation of this set of EGFR mutants likely represents intrinsic activation because of internal deletions of carboxyl terminal segments.

Because the kinase domain of WT-EGFR is intrinsically autoinhibited, and a ligand-induced dimerization promotes its activation (Zhang *et al.*, 2006), we investigated a model attributing basal activation of the EGFRvIV mutants to constitutive receptor dimerization. To this end, we used the more active EGFRvIVb mutant, which was analyzed in two stably expressing cell lines: murine NIH-3T3 fibroblasts and human U87MG glioma cells. To visualize receptor dimers, we incubated whole cell extracts with the covalent crosslinking reagent bis(sulfosuccinimidyl) suberate (BS3) as previously described (Shtiegman *et al.*, 2007). In addition, because of the low abundance of receptor dimers, we increased sensitivity of detection using antibodies to the phosphorylated form of tyrosine 1068 of EGFR. Exposure to EGF of either cell type expressing WT-EGFR verified the ability of BS[3] to capture the otherwise noncovalently associated, reversible receptor dimers, which are strictly dependent on ligand binding. In contrast, dimers of the EGFRvIII mutant were present independently of EGF stimulation (Figure 4c). Importantly, the EGFRvIVb mutant receptor expressed in either cell line showed small populations of basally phosphorylated dimers, which were dramatically enhanced after treatment with EGF. These observations imply that the more oncogenic EGFRvIII mutant exists primarily in constitutively active receptor dimers, whereas only a small fraction of EGFRvIVb exists in active dimers before ligand binding, which may explain the weaker transforming and autophosphorylating activities of this mutant.

Structural studies have shown that ligand-induced EGFR dimerization involves major domain rearrangements in the extracellular part, exposing a critical dimerization arm (Burgess *et al.*, 2003). Because the observed constitutive dimerization of this mutant is likely independent of the dimerization arm. To test this hypothesis we introduced a point mutation (replacement of a glutamate at position 293) in EGFRvIVa, EGFRvIVb and WT-

EGFR, which impairs formation of receptor dimers mediated through intermolecular interactions of the extracellular domains (Dawson *et al.*, 2005). The mutant receptors were transiently expressed in CHO (Chinese hamster ovary) cells, which enable high ectopic expression on an EGFR-null background. As we previously reported (Tzahar *et al.*, 1996), when overexpressed in CHO cells, WT-EGFR shows weak tyrosine phosphorylation before stimulation. Nevertheless, this basal activity was markedly enhanced on EGF treatment (Figure 4d). Remarkably, the glutamate-to-alanine mutation (E293A) completely abolished both basal and EGF-inducible tyrosine phosphorylation of WT-EGFR, in line with a requirement of extracellular domain interfaces for receptor dimerization of WT-EGFR (Dawson *et al.*, 2005). As expected, both EGFRvIV mutants showed high basal phosphorylation when overexpressed in CHO cells, but this was not abolished in the respective E293A mutant forms (Figure 4d). In conclusion, the EGFRvIVb mutant of EGFR shows relatively high basal phosphorylation, which might be attributed to an intrinsic ability to form dimers before stimulation with EGF. This intrinsic propensity to dimerize is independent of the extracellular dimerization arm of EGFR, but may involve the mutated regions within the cytoplasmic portion of EGFRvIV receptors (see Discussion).

HSP90 regulates stability and activity of the EGFRvIV mutants

Using virally infected murine fibroblasts and human U87MG cells, we observed consistently higher expression of all mutant forms of EGFR compared with WT receptor, despite uniformity of experimental conditions. Hence, we hypothesized that a post-translational mechanism leads to increased stability of mutant EGFRs. It has previously been shown that constitutively active and oncogenic forms of tyrosine kinases, such as p210BCR-ABL and v-SRC, are more stringently controlled by HSP90 than their normal cellular counterparts, c-ABL and c-SRC (An *et al.*, 2000). This observation extends to mutant forms of EGFR frequently detected in non-small cell lung cancer: mutational activation of several distinct forms is associated with relatively high basal phosphorylation (Shtiegman *et al.*, 2007), and with increased dependence on HSP90 for stability (Shimamura *et al.*, 2005). These considerations predict that HSP90 controls the stability of the EGFRvIV mutants more stringently than it regulates WT-EGFR. Consistent with this prediction, after treatment with 17-AAG, a specific HSP90 inhibitor (Chiosis *et al.*, 2003), NIH-3T3 cells stably expressing the vIVb mutant partly lost their transformed phenotype and reverted to a morphology that is similar to the phenotype of WT-EGFR-expressing cells (Figure 5a). This property was shared by EGFRvIII, a mutant known to be regulated by HSP90 (Lavictoire *et al.*, 2003). In line with these observations, after 24 h of HSP90 inhibition, the levels of both EGFRvIV mutant proteins, similar to the levels of EGFRvIII, significantly decreased, but the level of WT-EGFR remained largely unaffected, further supporting a stabilizing role toward mutant receptors. Concomitantly, 17-AAG reduced tyrosine phosphorylation of all three types of EGFR deletion mutants, under both basal and EGF-stimulated conditions (Figure 5b). In line with this observation, crosslinking analyses of monomeric and dimeric forms of the vIII and vIVb mutant forms of EGFR reflected reduced overall phosphorylation, and raised the possibility that the dimeric form might be more sensitive to 17-AAG than the monomeric species of both mutants (Supplementary Figure S3A). Taken together with the inferred necessity for basal tyrosine phosphorylation and sensitivity to a kinase inhibitor (Figure 1c), the results obtained with 17-AAG imply that the transforming potential of the EGFRvIV mutants might critically depend not only on the catalytic kinase activity but also on stabilization by HSP90. This possibility is supported by the experiment presented in Supplementary Figure S3B: a combination of sub-optimal concentrations of 17-AAG and AG1478 more effectively normalized the morphology of EGFRvIV-expressing fibroblasts. If extended to animal models, our biochemical and cellular observations may identify kinase and chaperone blockers as potential treatment strategies for a subgroup of patients with brain tumors.

Discussion

Overexpression of EGFR is one of the most frequently diagnosed genetic aberrations of glioblastomas, and is often accompanied by deletion mutations. The most frequently detected and best-studied deletion mutant is EGFRvIII (Gan *et al.*, 2009). This mutated receptor is highly oncogenic and shares both structural and functional similarities with the viral EGFR homolog, v-ErbB (Shu *et al.*, 1991). The two EGFRvIV mutants, termed EGFRvIVa and EGFRvIVb in this study, have so far evaded biochemical investigation. These mutants lack a significant segment of their noncatalytic carboxyl terminal sequences, yet their extracellular domain is intact. Interestingly, a similar deletion was uncovered in the S3v-ErbB strain of the avian erythroblastosis virus, which is more aggressive than other strains (McManus *et al.*, 1997).

Our results indicate that the internal deletions of EGFRvIV enhance basal kinase activity, and confer oncogenic phenotypes. In addition, we show that the signaling pathways induced by these mutations differ from those activated by EGFRvIII. Despite differences, EGFRvIV and EGFRvIII share some similarities. For example, both activate AKT and decrease phosphorylation of a negative regulator, EPHA2 (Figure 3). This uncoupling of a negative feedback loop potentially enhances the transforming receptors. An additional common property of EGFRvIII and EGFRvIV is their dependence on the chaperoning activity of HSP90 (Figure 5), which explains the higher abundance of mutated EGFRs relative to WT. Finally, our results suggest that similar to the case of EGFRvIII, basal dimerization may be involved in EGFRvIV activation (Figure 4c). Nevertheless, although relief of extracellular constraints might contribute to dimerization of EGFRvIII, our data favor involvement of the kinase domain in basal dimerization of EGFRvIV (Figure 4c). It is notable, however, that the fraction of pre-dimerized EGFRvIII exceeds the portion of EGFRvIV molecules present within dimers, before EGF binding.

Other receptor tyrosine kinases are regulated by their C-tails (Shewchuk *et al.*, 2000; Chiara *et al.*, 2004). However, because of its unique independence of phosphorylation within the activation loop (Gotoh *et al.*, 1992) and because of the fact that the kinase domain of EGFR does not require large spatial rearrangements to achieve activation (Stamos *et al.*, 2002), catalytic regulation of this receptor is distinct. On the basis of the structural and computational analyses, Landau *et al.* (2004) suggested that a negatively charged segment (residues 979–996) of the carboxyl terminal region of EGFR forms large complementary surfaces with the kinase domain and, thereby, may inhibit its catalytic activity. Furthermore, although they differ in conformation, two crystal structures documented physical interactions between the kinase domain and carboxyl terminal segments of EGFR: the first report entails an inactive kinase stabilized by lapatinib, a tyrosine kinase inhibitor (Wood *et al.*, 2004; see an illustration in Supplementary Figure S4A). Accordingly, two α-helical regions, 971–980 and 983–990, bind to the kinase domain, potentially inhibiting its activation. The other structure suggested interactions *in trans*, in which the C-tail of one receptor molecule interacts with the kinase of the other receptor, thereby stabilizing an inactive dimer (Jura *et al.*, 2009) (Supplementary Figure S4B). This inactive conformation is thought to hinder a kinase–juxtamembrane contact, which is essential for subsequent activation and kinase–kinase interaction. Taken together, both computational and crystallographic analyses lend support to the prediction that the naturally occurring EGFRvIV mutants lack a kinase-inhibitory region, thereby attaining enhanced constitutive enzymatic activities.

In summary, we conclude that the C-tail distal to the kinase domain of EGFR possesses an inhibitory role, which interferes with catalytic activation in the absence of ligand-induced dimerization. Upon deletion in brain tumors, mutant EGFRs acquire basal tyrosine

phosphorylation that instigates unique sets of signaling proteins, and culminates in malignant transformation (see model in Figure 6). Intriguingly, the shorter deletion mutant, namely EGFRvIVb, consistently showed higher kinase and oncogenic activities than the longer deletion mutant, EGFRvIVa. Future mutational studies will resolve these differences, along with pinpointing the exact amino acids necessary for kinase regulation.

Materials and methods

Plasmid construction and mutagenesis

A pCDNA3 plasmid containing the complementary DNA of human EGFR was mutated using QuikChange (Stratagene, La Jolla, CA, USA), with protocol adaptations. In short, deletions were generated using two primers out-flanking the sequence to be deleted. After a PCR reaction, DPN I was added, DNA was purified using a PCR purification kit (Qiagene, Hilden, Germany) and incubated for 30 min with polynucleotide kinase and ATP (Roche, Mannheim, Germany). The DNA was purified and ligated using T4-DNA ligase. Thereafter, mutant DNA segments were cloned into the retroviral pLXSN vector and pre-cleaved with the restriction enzymes BglII and XhoI. pLXSN-V12HRAS was a generous gift from Julian Downward (London Research Institute, UK). pLRNL-WT-EGFR and U87MG cells were a generous gift from Frank Furnari (University of California, San Diego, CA, USA).

Gene transfer procedures

Transient plasmid expression was achieved using Lipofectamine (Invitrogen, Carlsbad, CA, USA). For stable ectopic expression, HEK-293 cells were co-transfected with pLXSN or pLRNL (5 μg) and a viral packaging plasmid (5 μg). Virus-containing medium was collected 48 h after transfection, mixed with hexadimethrine bromide (5 μg/ml), and the mixture was incubated with cells for 24 h. Cells were maintained in normal medium for additional 24 h, followed by selection under G418 (from Gibco BRL, Grand Island, NY, USA; 500 or 600 μg/ml, respectively).

Cell lines and treatments with specific inhibitors

Cells were maintained in Dulbecco's modified Eagle's medium (Gibco Life Technologies, Paisley, UK), supplemented with 10% heat-inactivated fetal calf serum. Cells were incubated with the EGFR kinase inhibitor, AG1478 (1 μM), or with the HSP90 inhibitor, 17-AAG (50 n$_M$; Calbiochem, Gibbstown, NJ, USA), in growth medium for 4 days. The medium of the 17-AAG-treated cells was refreshed daily.

Cell proliferation assay

NIH-3T3 cells were plated in 24-well plates (8000 cells/well), in triplicates. After variable length incubation, cells were fixed with methanol at −20 °C for 4 min. After methanol removal, 1ml of methyl violet (0.3%) was added for 20 min at −20 °C. Plates were washed thoroughly under water and air-dried. Finally, cells were dissolved in 0.2 ml solution of 1N NaOH and 1% Na-dodecylsulphate, and light absorbance was determined at 570 nm.

Anchorage-independent growth assay

After solidification of a base layer containing growth medium and 0.5% bactoagar (Conda Laboratories, Madrid, Spain), a mixture of medium, bactoagar (0.42%) and cells (2000) was spread in triplicates. Digital images were taken after 3 weeks of incubation. Colony coverage area was calculated using the ImageJ software (NIH, Bethesda, MD, USA, http://rsb.info.nih.gov/ij/).

Tumor growth in animals

NIH-3T3 cells (2×10^6 cells per animal) were injected subcutaneously into nude mice (CD-1-Hfh11-nu; 6-week-old females). Tumor formation was routinely checked and all mice were killed when the first tumors reached approximately 10% of the total body weight.

Sample preparation, peptide immunoprecipitation and mass spectrometry analyses

In all, 5 million cells were seeded in 15-cm dishes, incubated for 24 h and then serum starved for 12 h before either treatment without or with EGF (10 ng/ml) for 10 min. For each of the two biological replicates performed, cells were lysed in 8 M urea and subjected to reduction, alkylation and trypsin digestion as previously described (Huang et al., 2007). Peptides were desalted on a C18 Sep-Pak Plus cartridge (Waters, Milford, MA, USA), eluted with 25% acetonitrile and lyophilized to dryness, Milford, MA, USA. Lyophilized peptides were subjected to labeling with the iTRAQ 8-plex reagent (Applied Biosystems, Foster City, CA, USA). Peptide immunoprecipitation was performed as described (Huang et al., 2007). Immobilized metal affinity chromatography was performed to enrich for phosphorylated peptides, and peptides retained on the column were eluted with 250 mM sodium phosphate (pH 8.0) and analyzed by electrospray ionization liquid chromatography tandem MS on a QqTof (QSTAR Elite, Applied Biosystems) as described (Huang et al., 2007).

Phosphopeptide sequencing, quantification and clustering

MS/MS spectra were extracted, searched and quantified using Protein Pilot (Applied Biosystems). Phosphorylation sites and peptide sequence assignments were validated by manual confirmation of raw MS/MS data. Peak areas of iTRAQ marker ions were normalized with values from the iTRAQ marker ion peak area of non-phosphorylated peptides in supernatant of the immunoprecipitation. The data in the Supplementary Excel File (two sheets) represent the mean and s.d. of phosphopeptides from two biological replicates normalized to WT-EGFR plus EGF (Supplementary Excel File, sheet 1). Next, signals corresponding to all phosphotyrosine-containing peptides from unstimulated samples were centered using the average signal of each peptide across all samples as reference. Samples were then grouped into three clusters using unsupervised coupled two-way clustering (Supplementary Excel File, sheet 2) (Getz et al., 2000).

Covalent crosslinking analyses

Cells were starved overnight in serum-free medium, and incubated at 37 1C with EGF (10 ng/ml, unless stated otherwise) for the indicated time intervals. For covalent crosslinking assays, cells were grown on 10-cm plates, treated with EGF and washed twice with saline. Thereafter, cells were harvested and incubated for 20 min on ice in lysis buffer containing 2 mM BS³ (Pierce, Rockford, IL, USA). The reaction was quenched by adding glycine (50 mM, final concentration).

Supplementary Material

Refer to Web version on PubMed Central for supplementary material.

Acknowledgments

References

An WG, Schulte TW, Neckers LM. The heat shock protein 90 antagonist geldanamycin alters chaperone association with p210bcrabl and v-src proteins before their degradation by the proteasome. Cell Growth Differ. 2000; 11:355–360. [PubMed: 10939589]

Burgess AW, Cho HS, Eigenbrot C, Ferguson KM, Garrett TP, Leahy DJ, et al. An open-and-shut case? Recent insights into the activation of EGF/ErbB receptors. Mol Cell. 2003; 12:541–552. [PubMed: 14527402]

Chiara F, Bishayee S, Heldin CH, Demoulin JB. Autoinhibition of the platelet-derived growth factor beta-receptor tyrosine kinase by its C-terminal tail. J Biol Chem. 2004; 279:19732–19738. [PubMed: 14996833]

Chiosis G, Huezo H, Rosen N, Mimnaugh E, Whitesell L, Neckers L. 17AAG: low target binding affinity and potent cell activity– finding an explanation. Mol Cancer Ther. 2003; 2:123–129. [PubMed: 12589029]

Clarkson RW, Boland MP, Kritikou EA, Lee JM, Freeman TC, Tiffen PG, et al. The genes induced by signal transducer and activators of transcription (STAT)3 and STAT5 in mammary epithelial cells define the roles of these STATs in mammary development. Mol Endocrinol. 2006; 20:675–685. [PubMed: 16293640]

Dawson JP, Berger MB, Lin CC, Schlessinger J, Lemmon MA, Ferguson KM. Epidermal growth factor receptor dimerization and activation require ligand-induced conformational changes in the dimer interface. Mol Cell Biol. 2005; 25:7734–7742. [PubMed: 16107719]

Ekstrand AJ, Sugawa N, James CD, Collins VP. Amplified and rearranged epidermal growth factor receptor genes in human glioblastomas reveal deletions of sequences encoding portions of the N- and/or C-terminal tails. Proc Natl Acad Sci USA. 1992; 89:4309–4313. [PubMed: 1584765]

Frederick L, Wang XY, Eley G, James CD. Diversity and frequency of epidermal growth factor receptor mutations in human glioblastomas. Cancer Res. 2000; 60:1383–1387. [PubMed: 10728703]

Gan HK, Kaye AH, Luwor RB. The EGFRvIII variant in glioblastoma multiforme. J Clin Neurosci. 2009; 16:748–754. [PubMed: 19324552]

Getz G, Levine E, Domany E. Coupled two-way clustering analysis of gene microarray data. Proc Natl Acad Sci USA. 2000; 97:12079–12084. [PubMed: 11035779]

Gotoh N, Tojo A, Hino M, Yazaki Y, Shibuya M. A highly conserved tyrosine residue at codon 845 within the kinase domain is not required for the transforming activity of human epidermal growth factor receptor. Biochem Biophys Res Commun. 1992; 186:768–774. [PubMed: 1323290]

Hafizi S, Dahlback B. Signalling and functional diversity within the Axl subfamily of receptor tyrosine kinases. Cytokine Growth Factor Rev. 2006; 17:295–304. [PubMed: 16737840]

Huang PH, Mukasa A, Bonavia R, Flynn RA, Brewer ZE, Cavenee WK, et al. Quantitative analysis of EGFRvIII cellular signaling networks reveals a combinatorial therapeutic strategy for glioblastoma. Proc Natl Acad Sci USA. 2007; 104:12867–12872. [PubMed: 17646646]

Huang PH, Xu AM, White FM. Oncogenic EGFR signaling networks in glioma. Sci Signal. 2009; 2:re6. [PubMed: 19738203]

Hynes NE, MacDonald G. ErbB receptors and signaling pathways in cancer. Curr Opin Cell Biol. 2009; 21:177–184. [PubMed: 19208461]

Jeuken J, Sijben A, Alenda C, Rijntjes J, Dekkers M, Boots-Sprenger S, et al. Robust detection of EGFR copy number changes and EGFR variant III: technical aspects and relevance for glioma diagnostics. Brain Pathol. 2009; 19:661–671. [PubMed: 19744038]

Jura N, Endres NF, Engel K, Deindl S, Das R, Lamers MH, et al. Mechanism for activation of the EGF receptor catalytic domain by the juxtamembrane segment. Cell. 2009; 137:1293–1307. [PubMed: 19563760]

Katz M, Amit I, Yarden Y. Regulation of MAPKs by growth factors and receptor tyrosine kinases. Biochim Biophys Acta. 2007; 1773:1161–1176. [PubMed: 17306385]

Kuan CT, Wikstrand CJ, Bigner DD. EGF mutant receptor vIII as a molecular target in cancer therapy. Endocr Relat Cancer. 2001; 8:83–96. [PubMed: 11397666]

Ladanyi M, Pao W. Lung adenocarcinoma: guiding EGFRtargeted therapy and beyond. Mod Pathol. 2008; 21(Suppl 2):S16–S22. [PubMed: 18437168]

Landau M, Fleishman SJ, Ben-Tal N. A putative mechanism for downregulation of the catalytic activity of the EGF receptor via direct contact between its kinase and C-terminal domains. Structure. 2004; 12:2265–2275. [PubMed: 15576039]

Lavictoire SJ, Parolin DA, Klimowicz AC, Kelly JF, Lorimer IA. Interaction of Hsp90 with the nascent form of the mutant epidermal growth factor receptor EGFRvIII. J Biol Chem. 2003; 278:5292–5299. [PubMed: 12471035]

Li JJ, Liu DP, Liu GT, Xie D. EphrinA5 acts as a tumor suppressor in glioma by negative regulation of epidermal growth factor receptor. Oncogene. 2009; 28:1759–1768. [PubMed: 19270726]

McManus MJ, Lingle WL, Salisbury JL, Maihle NJ. A transformation-associated complex involving tyrosine kinase signal adapter proteins and caldesmon links v-erbB signaling to actin stress fiber disassembly. Proc Natl Acad Sci USA. 1997; 94:11351–11356. [PubMed: 9326613]

Nagane M, Coufal F, Lin H, Bogler O, Cavenee WK, Huang HJ. A common mutant epidermal growth factor receptor confers enhanced tumorigenicity on human glioblastoma cells by increasing proliferation and reducing apoptosis. Cancer Res. 1996; 56:5079–5086. [PubMed: 8895767]

Pulciani S, Santos E, Lauver AV, Long LK, Barbacid M. Transforming genes in human tumors. J Cell Biochem. 1982; 20:51–61. [PubMed: 6761348]

Ramnarain DB, Park S, Lee DY, Hatanpaa KJ, Scoggin SO, Otu H, et al. Differential gene expression analysis reveals generation of an autocrine loop by a mutant epidermal growth factor receptor in glioma cells. Cancer Res. 2006; 66:867–874. [PubMed: 16424019]

Shewchuk LM, Hassell AM, Ellis B, Holmes WD, Davis R, Horne EL, et al. Structure of the Tie2 RTK domain: self-inhibition by the nucleotide binding loop, activation loop, and C-terminal tail. Structure. 2000; 8:1105–1113. [PubMed: 11080633]

Shimamura T, Lowell AM, Engelman JA, Shapiro GI. Epidermal growth factor receptors harboring kinase domain mutations associate with the heat shock protein 90 chaperone and are destabilized following exposure to geldanamycins. Cancer Res. 2005; 65:6401–6408. [PubMed: 16024644]

Shtiegman K, Kochupurakkal BS, Zwang Y, Pines G, Starr A, Vexler A, et al. Defective ubiquitinylation of EGFR mutants of lung cancer confers prolonged signaling. Oncogene. 2007; 26:6968–6978. [PubMed: 17486068]

Shu HK, Pelley RJ, Kung HJ. Dissecting the activating mutations in v-erbB of avian erythroblastosis virus strain R. J Virol. 1991; 65:6173–6180. [PubMed: 1681117]

Stamos J, Sliwkowski MX, Eigenbrot C. Structure of the epidermal growth factor receptor kinase domain alone and in complex with a 4-anilinoquinazoline inhibitor. J Biol Chem. 2002; 277:46265–46272. [PubMed: 12196540]

Tzahar E, Waterman H, Chen X, Levkowitz G, Karunagaran D, Lavi S, et al. A hierarchical network of interreceptor interactions determines signal transduction by Neu differentiation factor/neuregulin and epidermal growth factor. Mol Cell Biol. 1996; 16:5276–5287. [PubMed: 8816440]

Wong AJ, Bigner SH, Bigner DD, Kinzler KW, Hamilton SR, Vogelstein B. Increased expression of the epidermal growth factor receptor gene in malignant gliomas is invariably associated with gene amplification. Proc Natl Acad Sci USA. 1987; 84:6899–6903. [PubMed: 3477813]

Wood ER, Truesdale AT, McDonald OB, Yuan D, Hassell A, Dickerson SH, et al. A unique structure for epidermal growth factor receptor bound to GW572016 (Lapatinib): relationships among protein conformation, inhibitor off-rate, and receptor activity in tumor cells. Cancer Res. 2004; 64:6652–6659. [PubMed: 15374980]

Wykosky J, Gibo DM, Stanton C, Debinski W. EphA2 as a novel molecular marker and target in glioblastoma multiforme. Mol Cancer Res. 2005; 3:541–551. [PubMed: 16254188]

Zenz R, Wagner EF. Jun signalling in the epidermis: from developmental defects to psoriasis and skin tumors. Int J Biochem Cell Biol. 2006; 38:1043–1049. [PubMed: 16423552]

Zhang X, Gureasko J, Shen K, Cole PA, Kuriyan J. An allosteric mechanism for activation of the kinase domain of epidermal growth factor receptor. Cell. 2006; 125:1137–1149. [PubMed: 16777603]

Zhang Y, Wolf-Yadlin A, Ross PL, Pappin DJ, Rush J, Lauffenburger DA, et al. Time-resolved mass spectrometry of tyrosine phosphorylation sites in the epidermal growth factor receptor signaling

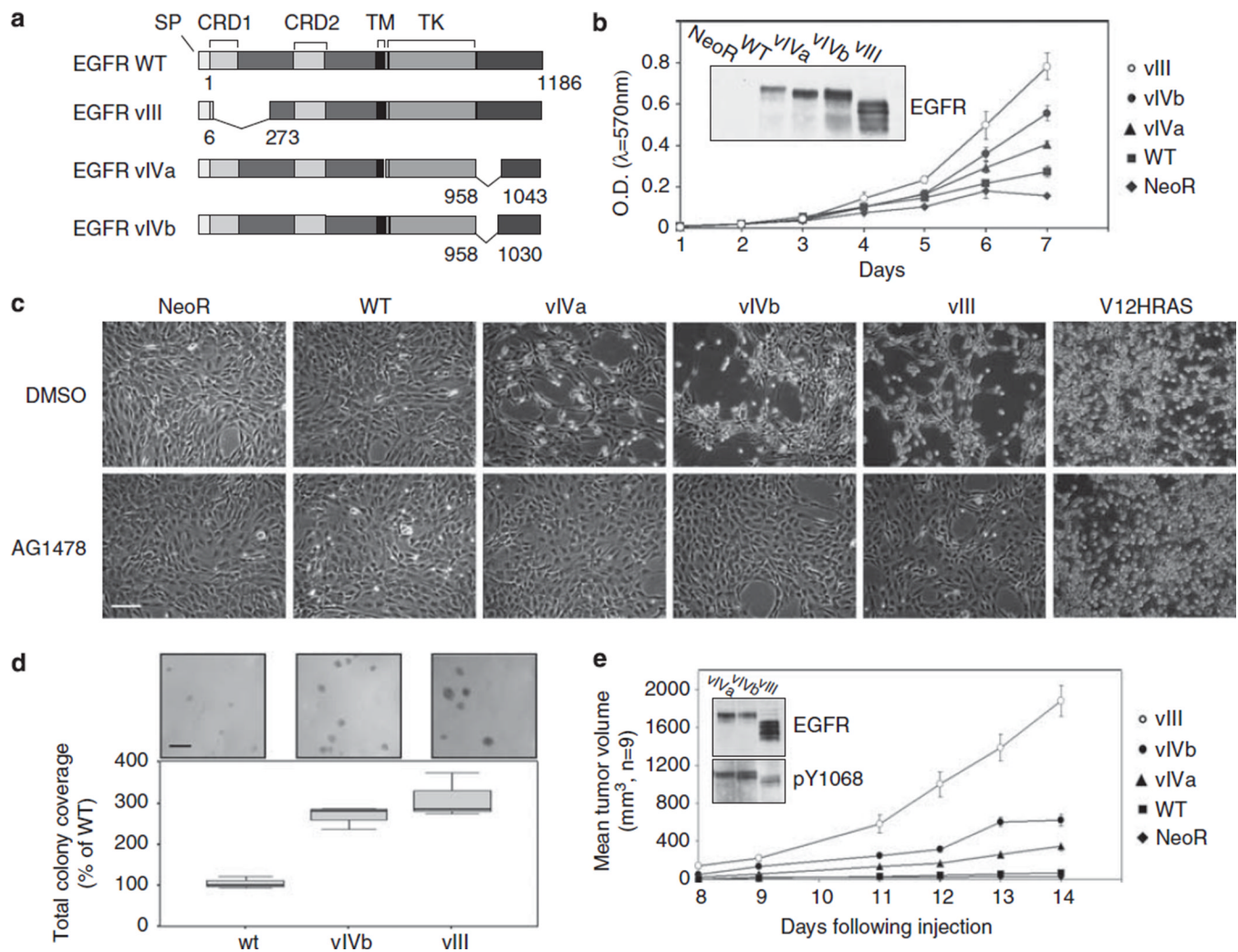network reveals dynamic modules. Mol Cell Proteomics. 2005; 4:1240–1250. [PubMed: 15951569]

Figure 1.
Transforming activities of the EGFRvIV deletion mutants. (**a**) Schematic representation of the EGFR deletion mutations that are the main focus of this study. Amino acid numbers are indicated, along with mutants' names. (**b**) NIH-3T3 cells stably expressing the indicated forms of EGFR (or a vector control; *NeoR*) were grown for the indicated time intervals and stained with methyl violet. Optical density was measured after dye dissolution. Averages ± s.d. (bars) are shown. Inset: an immunoblot of whole lysates of the indicated NIH-3T3 cell derivatives using an anti-EGFR antibody. (**c**) NIH-3T3 cells expressing the indicated EGFR mutants were incubated with either AG1478 (1 μM) or with dimethylsulfoxide (DMSO) as solvent control. Cells were incubated for 5 days before digital images were taken. Scale bar = 50 μm. (**d**) Murine fibroblasts stably expressing the indicated forms of EGFR were plated in a mixture of agar and medium. Shown images were captured 5 weeks later. Colony coverage was measured using the ImageJ software. Each box plot is composed of five horizontal lines that show the 10th, 25th, 50th, 75th and 90th percentiles of the respective sample. Scale bar=0.5 mm. (e) The indicated stable derivatives of NIH-3T3 cells were injected subcutaneously into nude mice (2×10^6 cells/animal) and tumor volumes were measured. Averages ± s.e. (bars) are shown. Inset: an immunoblot of whole lysates of the indicated NIH-3T3 cell derivatives using an anti-EGFR antibody and an antibody to

phosphorylated tyrosine 1068 of EGFR. SP, signal peptide; CRD, cysteine-rich domain; TM, transmembrane; TK, tyrosine kinase.
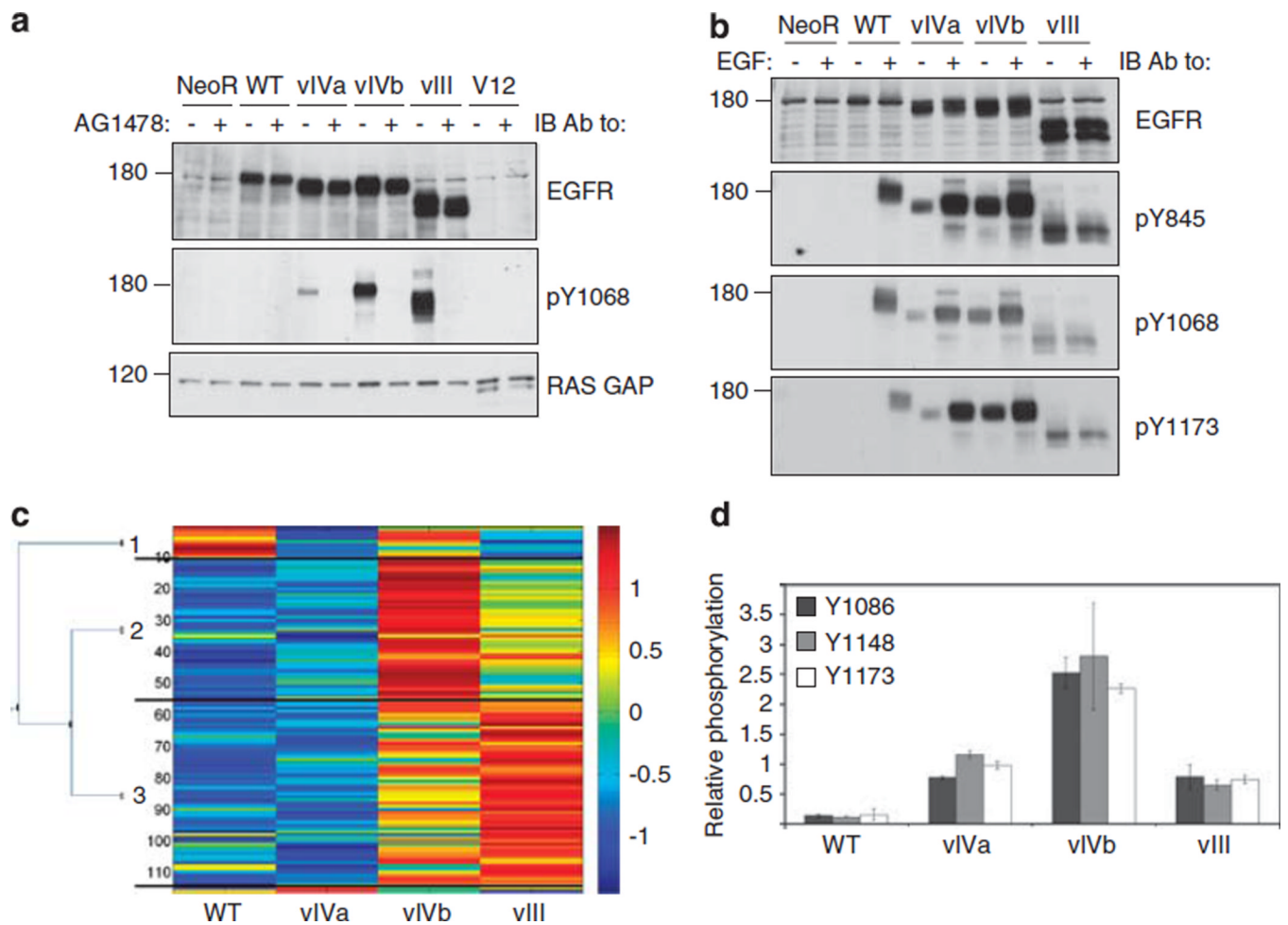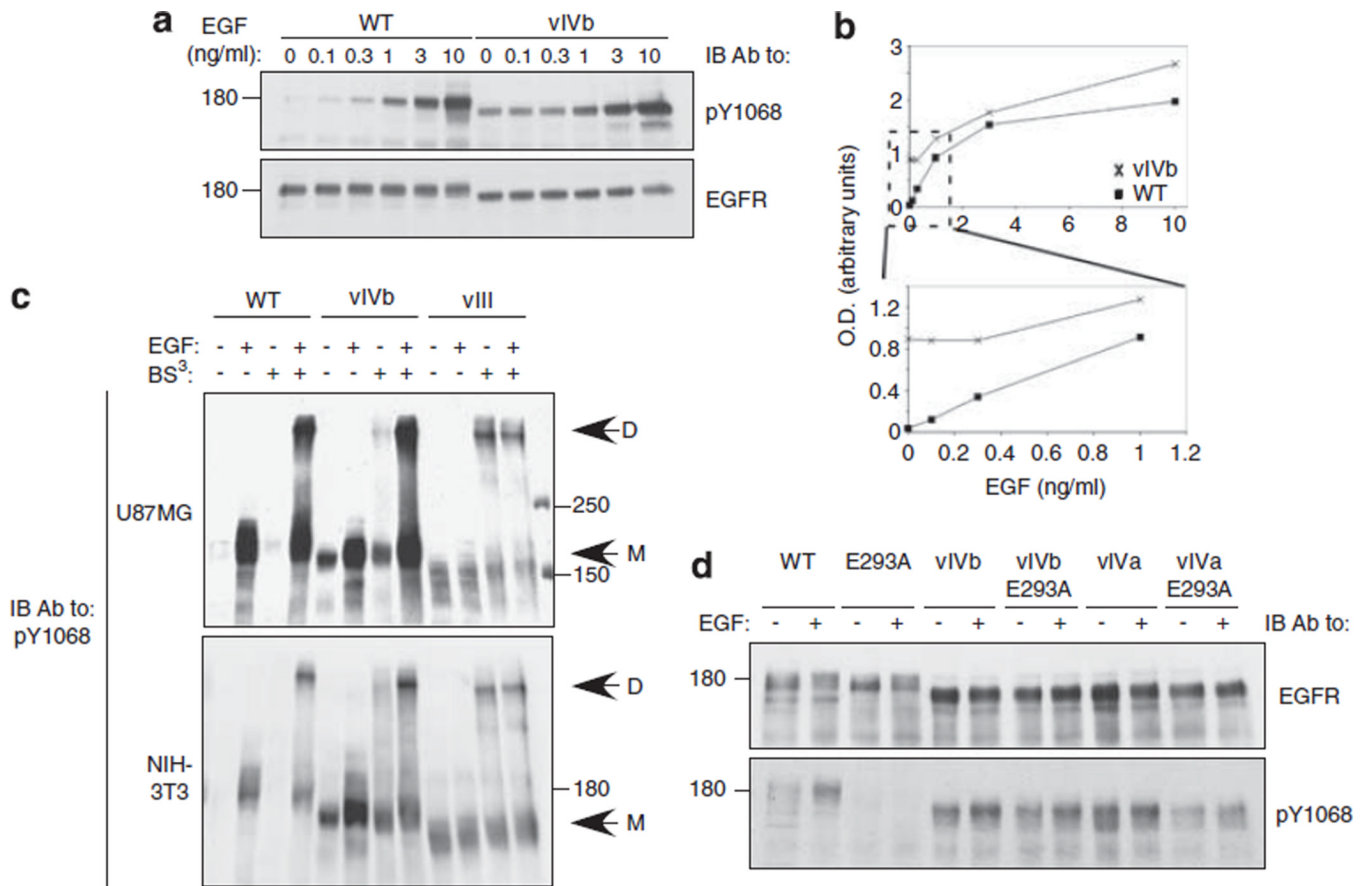
Figure 2.
The EGFRvIV mutants are basally phosphorylated. (**a**) The cells from the experiment shown in Figure 1c were extracted and subjected to immunoblotting using the indicated antibodies. (**b**) NIH-3T3 cells expressing the indicated EGFR mutants were incubated for 10 min without or with EGF (10 ng/ml), and the phosphorylation status of the indicated tyrosine residues of EGFR was determined by immunoblotting. (**c**) Murine fibroblasts ectopically expressing different forms of human EGFR were lysed, whole extracts were processed and MS/MS spectra obtained as detailed under Materials and methods. Centered signals of all phosphotyrosine-containing peptides of the cells were grouped into the indicated three clusters (see Materials and methods). See Supplementary Excel File (sheet 2). (**d**) Three EGFR tyrosine phosphorylation sites were identified by LC/MS/MS: Y1086, Y1148 and Y1173. The relative phosphorylation levels of the various EGFR forms in the basal state are indicated.
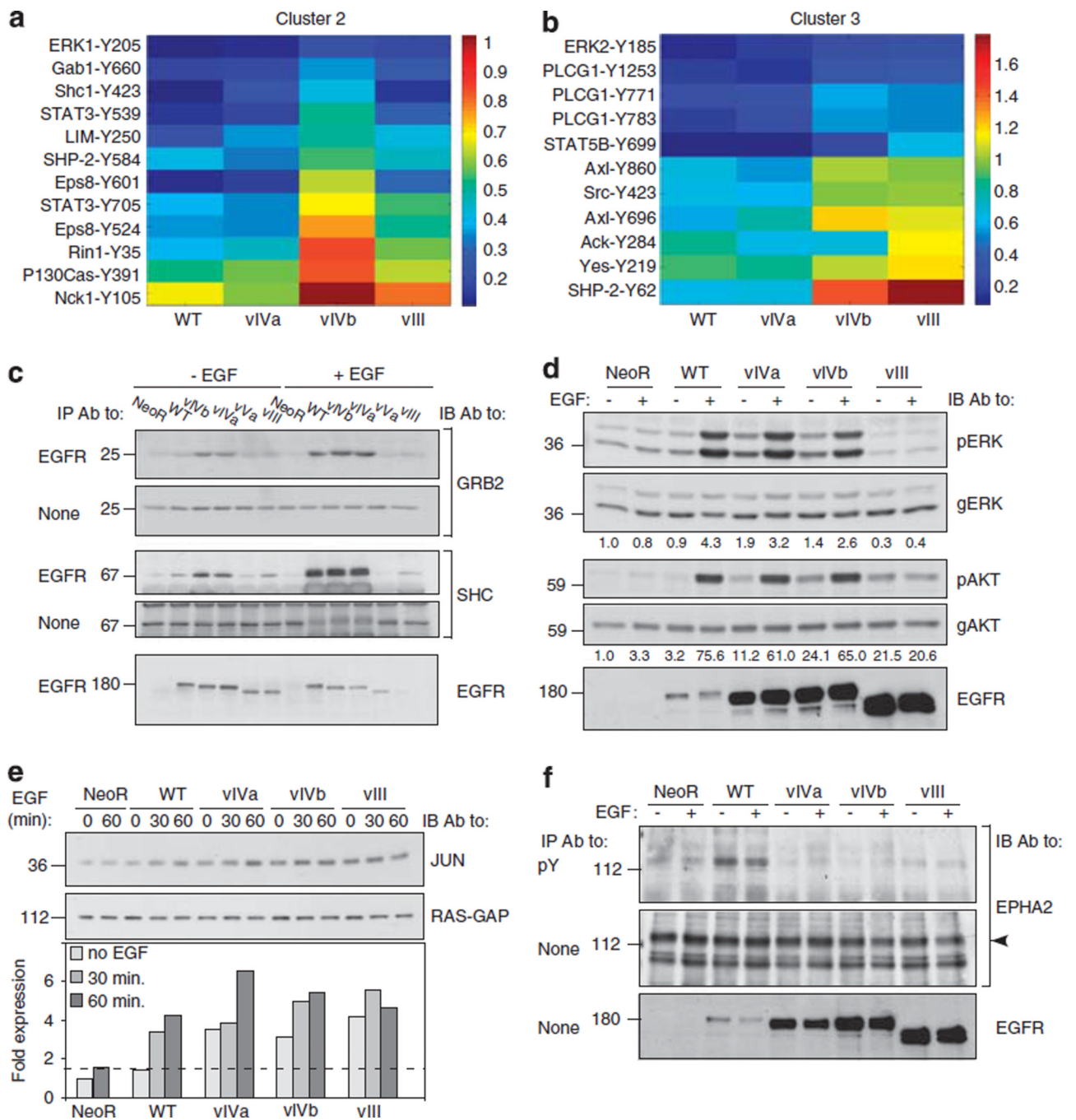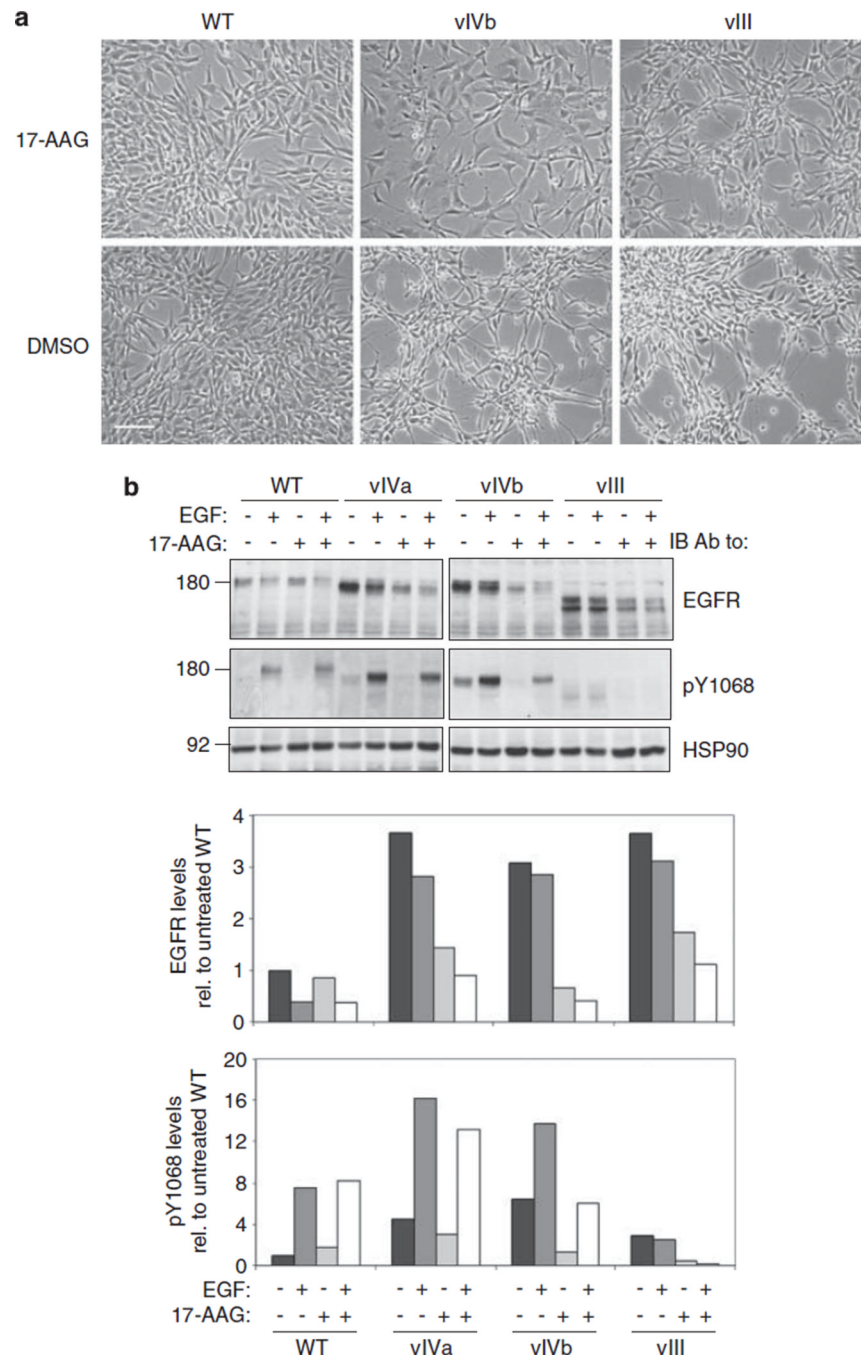
Figure 3.
Constitutive signaling by the EGFRvIV mutants. (**a, b**) Murine fibroblasts ectopically expressing the indicated forms of EGFR were subjected to phosphoproteomic analyses, and phosphorylation levels of signaling and adaptor proteins presented as heatmaps. Listed are specific tyrosine phosphorylation sites of substrates assigned to clusters 2 and 3. SeeSupplementary Excel File (sheet 1). (**c**) NIH-3T3 cells expressing the indicated EGFR mutants were incubated for 10 min without or with EGF. Cell lysates were subjected to immunoprecipitation (IP) using an antibody to EGFR and immunoblotting (IB) using antibodies specific to the adaptor proteins SHC and GRB2. Whole cell extracts were also

analyzed. (**d**) NIH-3T3 cells expressing the indicated EGFR mutants were incubated for 10 min without or with EGF. Cell lysates were subjected to IB using antibodies to the general and the phosphorylated forms (pERK and pAKT) of extracellular signal-regulated kinase (ERK) and AKT. Numbers indicate normalized intensities of phosphorylated bands. (**e**) NIH-3T3 cells expressing the indicated EGFR mutants were incubated without or with EGF (10 ng/ml) for the indicated intervals. The relative levels of JUN were determined by IB (upper panel). The bands were quantified and normalized according to RAS-GAP. The dashed line marks the basal level of JUN induction in WT-EGFR-expressing cells. (**f**) NIH-3T3 cells expressing the indicated EGFR forms were treated without or with EGF (10 ng/ml; 10 min). Cell lysates were subjected to IP with an antibody directed against phosphotyrosine (pY) and IB for the EPHA2 receptor.

Figure 4.
EGFRvIV shows constitutive, but partial, dimerization and autophosphorylation. (**a**) NIH-3T3 cells expressing either WT-EGFR or EGFRvIVb were incubated for 20 min with increasing EGF concentrations. Thereafter, the cells were extracted and analyzed by immunoblotting (IB) with the indicated antibodies. (**b**) Phospho-EGFR levels were derived from (**a**) by quantifying and normalizing band intensities. The lower panel enlarges the low range of EGF concentrations shown in the upper panel. (c) U87MG and NIH-3T3 cells stably expressing the indicated forms of ectopic EGFR were untreated or treated without or with EGF (10 ng/ml; 10 min). Whole cell extracts were prepared, cleared and incubated without or with a covalent crosslinking reagent, BS^3 (2 mM, 20 min), and subjected to immunoblotting analysis using an antibody specific to phosphorylated tyrosine 1068 of EGFR. *D* and *M* indicate EGFR dimers and monomers, respectively. (**d**) WT-EGFR and the EGFRvIV mutants were mutated at residue 293 (glutamate-to-alanine replacement). CHO cells were transfected with the indicated EGFR constructs, including double mutants carrying both the E293A mutation and a deletion, and incubated without or with EGF (10 ng/ml; 10 min). Whole cell extracts were immunoblotted with the indicated antibodies.

Figure 5.
The EGFRvIV mutants serve as clients of HSP90. (**a**) NIH-3T3 cells expressing the indicated forms of EGFR were incubated with either 17-AAG (50 nM; an HSP90 inhibitor) or with solvent (DMSO). Cells were incubated for 4 days before digital images were taken. Scale bar = 50 μm. (**b**) NIH-3T3 cells expressing the indicated EGFR mutants were incubated without or with 17-AAG (24 h; 50 nM) and without or with EGF (10 min). Cleared cell extracts were resolved by electrophoresis and immunoblotting with the indicated antibodies. The lower panels show quantification of total and phospho-EGFR levels, determined according to band intensities and normalization.
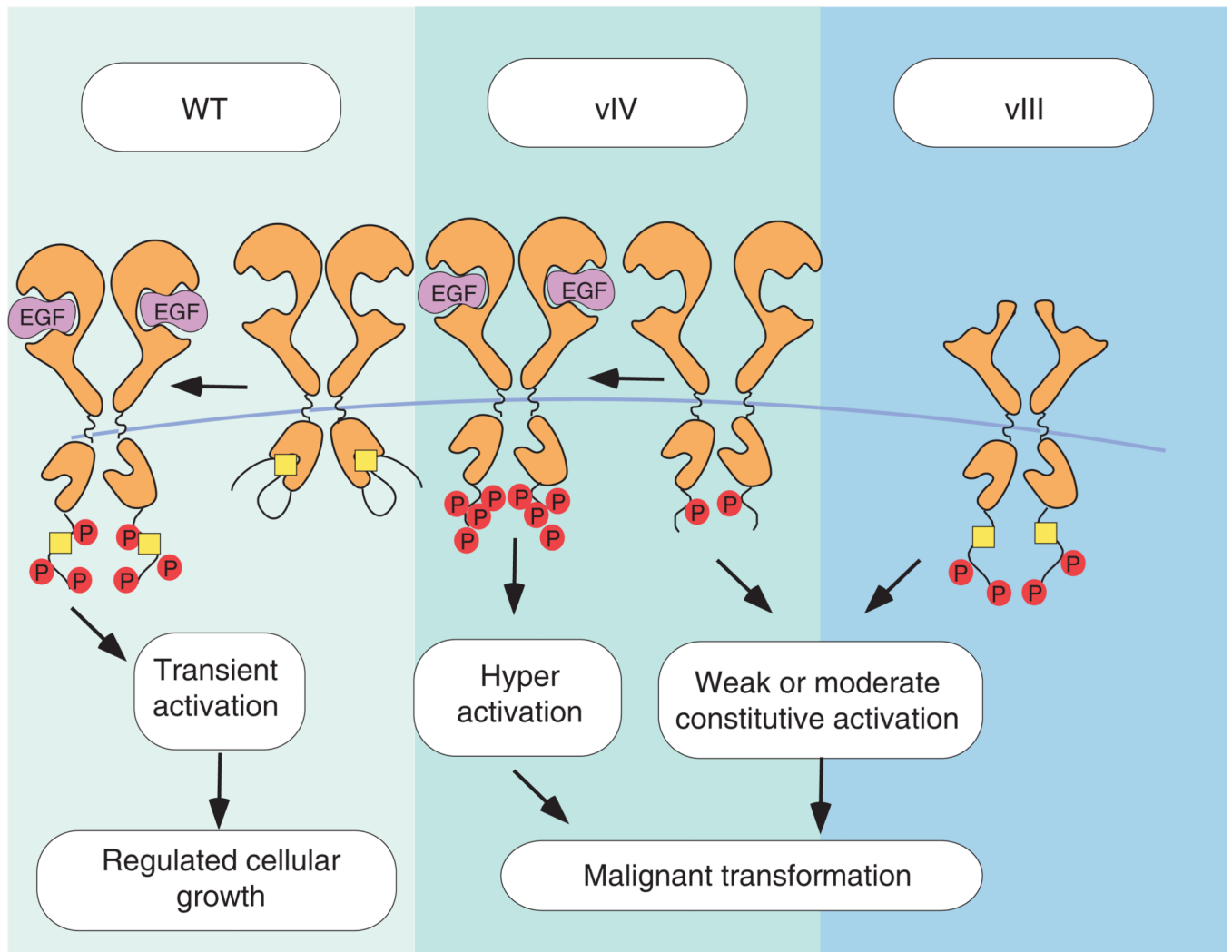
Figure 6.
A model that compares WT-EGFR and two oncogenic mutants, EGFRvIV and EGFRvIII. The red circles indicate phosphorylated tyrosine residues; the yellow rectangle marks the segment missing in the C-tail of EGFRvIV mutants. Unlike EGFRvIII, WT-EGFR and the EGFRvIV mutants can be stimulated by growth factors. On the other hand, both EGFRvIV and EGFRvIII show constitutive autophosphorylation that differentiates them from WT-EGFR and likely enhances aggressiveness of brain tumors.